Thickness Dependence of the Optical Properties of Ordered Silica-Air and Air-Polymer Photonic Crystals

Jane F. Bertone,[1] Peng Jiang,[1] Kevin S. Hwang,[1] Daniel M. Mittleman,[2] and Vicki L. Colvin[1,*]

[1]*Department of Chemistry and Center for Nanoscale Science and Technology, Rice University, MS-60, 6100 Main Street, Houston, Texas 77005*

[2]*Electrical and Computer Engineering, Rice University, MS-366, 6100 Main Street, Houston, Texas 77005*

(Received 25 March 1999)

We report observations of the optical stop band of periodic planar arrays of submicron silica spheres, and of macroporous polymers grown from these silica templates. The stop-band width and peak attenuation depend on the number of layers and on the dielectric contrast between the spheres and the interstitial regions, both of which are experimentally controlled. The results are compared to the predictions of the scalar wave approximation. This is the first systematic study of the thickness dependence of the stop band in colloidal photonic band gap structures.

PACS numbers: 42.70.Qs, 78.20.Ci, 81.05.Ys, 82.70.Dd

The optical properties of photonic band gap materials have been the subject of many experimental and theoretical studies in recent years [1]. In these systems the dielectric function is spatially periodic in one or more dimensions, and as a result their optical properties are dominated by strong diffraction effects. The propagation of light is strongly inhibited over a narrow range of frequencies; this produces a dip in the transmission spectrum known as a stop band. In order to construct structures whose stop bands are centered in the visible region, the length scale of the periodicity must shrink accordingly. As a result, lithographic fabrication of materials with visible stop bands is quite challenging.

One class of materials which offers a unique solution to this problem is colloidal crystals [2–5]. Here, one relies on the tendency of submicron dielectric spheres to spontaneously self-assemble into ordered arrays. This approach has several advantages over the conventional "top-down" fabrication techniques, including a wider versatility with respect to the choice of materials, the relative ease of casting high quality planar films as optical coatings, and the low cost of implementation. Further, colloids as small as 50 nm have been crystallized [6]; such systems could extend the applicability of photonic band gap materials into the soft-x-ray range. Finally, unlike lithographic and machining techniques, which generally limit sample thickness to only a few repeating layers, colloidal crystals can be fabricated with controlled thickness, up to hundreds of layers [7]. This may prove to be a significant advantage if control over sample thickness provides an avenue for tuning the optical properties.

Thus, an understanding of the evolution of the optical properties of these materials with an increasing number of layers is an important ingredient in the study of these strongly diffracting systems. Yet, a systematic investigation of this thickness dependence has been lacking. This is due to the difficulty in controlling the thickness of colloidal samples, and also in producing samples with sufficient uniformity and optical quality for such measurements. Although the thickness dependence of the optical properties of periodic dielectric media has been studied in the microwave and submillimeter range [8,9], these systems do not mimic the spherical close-packed arrangement common to most colloidal crystals.

In this work, we address this issue using colloidal crystals fabricated with a novel convective self-assembly process, which affords control over the sample thickness up to a hundred layers [10]. As the thickness of the colloidal crystal increases, the optical transmission spectrum changes in characteristic ways. The spectral position of the stop band is reasonably well described by Bragg's law. The peak optical density grows monotonically with the number of layers. More interesting behavior is found in the spectral width of the stop band. Controlling and understanding this width is important in the design of optical elements using these materials, including filters [7], lasers [11], and all-optical switches [12,13].

The samples used in this study are planar close-packed crystals of monodisperse silica spheres, containing few crystalline defects and virtually no grain boundaries. The silica spheres are grown using standard methods, with controllable diameters ranging from 200 to 400 nm [14]. Once grown, the silica/air composites can be used as templates for the growth of "inside-out" polymer films [15,16]. The interstitial regions of the silica film are filled with a low-viscosity monomer, which is then photopolymerized. When the silica is etched away, the remaining structure is a macroporous polymer, consisting of a close-packed array of air spheres. Because of the direct templating of the original silica film, the macroporous polymers maintain the high crystalline quality of the precursor silica films. Figure 1 shows edge-view electron micrographs of these samples. The insets show two-dimensional Fourier transforms of top-view large-area images, illustrating the high degree of crystalline order. The films are not

 0031-9007/99/83(2)/300(4)$15.00

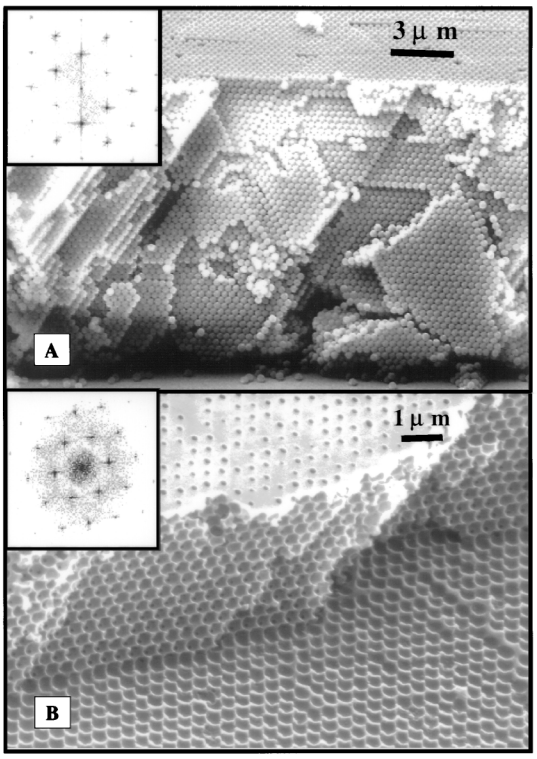

FIG. 1. (a) Scanning electron micrograph (SEM) edge view of a close-packed planar array of ~50 layers of silica spheres of ~295 nm diameter. The {111} crystal axis is oriented perpendicular to the substrate. (b) SEM edge view of a macroporous polymer film, consisting of a close-packed array of 13 layers of air spheres of ~330 nm diameter, with a polymer filling the interstitial regions. This sample has been formed using a silica crystal as a template, and thus maintains the high quality and crystalline orientation seen in Fig. 1(a). The insets show two-dimensional Fourier transforms of large-area (40×40 μm) top view images, illustrating the long-range order and registry of the crystal.

completely free of point defects; sphere vacancies are observed every ~10 μm. Significantly, grain boundaries are virtually never observed, and the crystal structure registry is preserved over a 1 cm^2 area [10].

The value of using these two types of samples lies in the range of control they afford over the dielectric contrast. The dielectric contrast ψ_0 can be defined in terms of the average dielectric of the medium, ε_0, and the dielectric of the interstitial regions, ε_{int}, according to $\psi_0 = (\varepsilon_0/\varepsilon_{\text{int}}) - 1$. Here, ε_0 is given by a weighted average: $\varepsilon_0 = \phi\varepsilon_{\text{sph}} + (1 - \phi)\varepsilon_{\text{int}}$, where ϕ is the volume fraction occupied by the spheres. For close-packed spheres, $\phi \approx 0.7405$. Films such as the one shown in Fig. 1(a) have a dielectric contrast of $\psi_0 \approx 0.66$. The macroporous polymer films, on the other hand, have negative contrasts, ranging from -0.33 to -0.5 depending on the index of the polymer. The ability to access a wide range of contrasts is valuable in assessing whether the optical properties are sample-specific, or are general features of close-packed arrays.

Optical transmission measurements are obtained at normal incidence to the film substrate, parallel to the {111} crystallographic axis, using a commercial UV-visible spectrometer. A smoothly varying monotonic background is subtracted from these spectra prior to further analysis. Although the origin of this background is unclear, it does not appear to be related to point defects or surface roughness. In any event, it varies only slightly in the vicinity of the optical stop band, and thus does not substantially influence the measurements. Typical normalized spectra are shown in Fig. 2. The inset shows the increase in the peak optical density with thickness. This increase is smooth and monotonic, and contains no evidence of a threshold thickness for the formation of a stop band.

In contrast, the width of the stop band displays a more dramatic dependence on film thickness. The observed narrowing of the stop band with increasing film thickness is reminiscent of the Debye-Scherrer effect in small crystallites [17]. Here, the angular width of a diffraction line is limited by the highest spatial frequency accessible in the reciprocal lattice. The width is thus inversely proportional to the number of lattice planes, and arbitrarily narrow lines should be obtained by increasing the crystal thickness. However, in the colloidal crystals studied here, the narrowing of the stop band saturates above a certain critical thickness. Further increases in film thickness do not result in narrower band widths.

This result is summarized in Fig. 3. Both types of sample reach their limiting bandwidths at thicknesses of ~10 layers. We note that these limiting values correspond to fractional bandwidths of ~5%. This is typical of the widths observed in colloidal crystals, but is much broader than the widths encountered in other types of diffraction phenomena. For example, single crystal x-ray linewidths [17] and reflection bandwidths of Bragg gratings in optical fibers [18] can both be as narrow as 0.01% of their spectral position. One possible explanation for the broad widths observed here is that defects dominate the optical response, and prevent the observation of narrower natural linewidths. This seems unlikely, given the high sample quality. Alternatively, the bandwidth may be an intrinsic property of these strongly diffracting systems.

To evaluate this issue, a simple model is used to calculate transmission spectra. There has been extensive theoretical work in recent years on the description of the photonic properties of periodic dielectric media [19]. One tractable analytic approach is the scalar wave approximation (SWA) [20,21]. Although this simple one-dimensional model has shortcomings [1,22], these difficulties are primarily related to its use in describing wave propagation along an *arbitrary* direction in the three-dimensional crystal. In the present work, we will be concerned solely with propagation along *high symmetry directions* of the crystal (i.e., the {111} axis). In this case, the one-dimensional SWA is appropriate. We note that

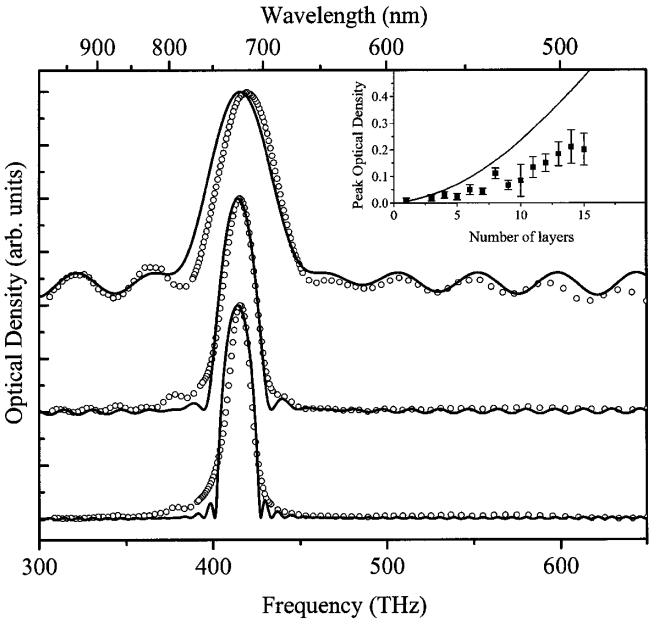

FIG. 2. Normal-incidence optical density spectra for samples such as those shown in Fig. 1(a) (circles). These spectra are of three different films of 342 nm silica spheres, with (from top to bottom) 9, 25, and 50 layers. The solid curves are calculated using the SWA. Both the data and the calculations have been scaled to uniform height and vertically offset for clarity. This overall multiplicative scaling is the only adjustable parameter in the calculation, since all other parameters (i.e., sphere diameter, material dielectric constants, number of layers) are determined by other measurements. The inset shows the monotonic increase in peak optical density with thickness for films of 295 nm spheres; the solid line shows the SWA prediction.

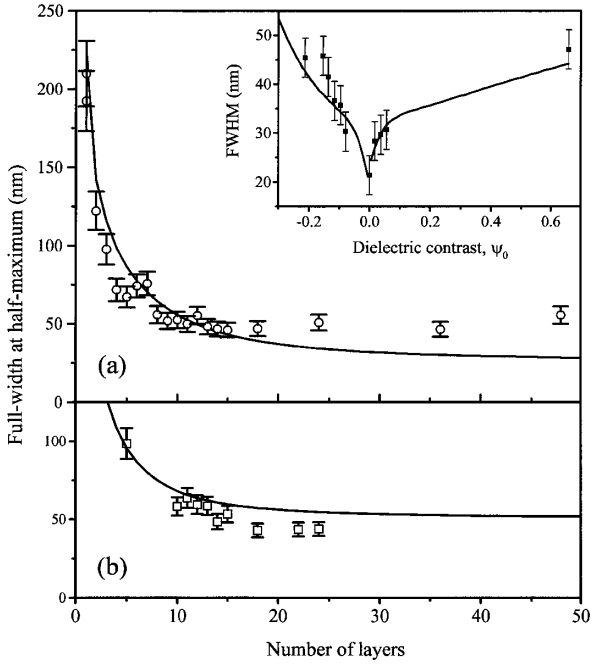

FIG. 3. Experimental and calculated stop-band widths as a function of the number of repeating layers. (a) Silica/air colloidal crystals, with a sphere diameter of 295 nm, and a dielectric contrast of $\psi_0 = 0.66$. (b) Air/polymer macroporous films, with air sphere diameter of 284 nm. The polymer in this case is poly-allyl methacrylate (PAMA), with a refractive index of $n = 1.64$, so these samples have $\psi_0 = -0.465$. The solid lines are calculated using the SWA, with no adjustable parameters. The inset shows the stop-band width for a single 20-layer colloidal crystal of 353 nm silica spheres, as a function of dielectric contrast ψ_0. The data point on the far right ($\psi_0 \sim 0.66$) is the width measured on the sample as grown, with air in the interstitial regions. The remaining ten points are extracted from the transmission spectra when the interstitial regions are filled with various nonabsorbing dielectric liquids. The calculated result from the SWA is shown as a solid line.

an analytic expression for the stop-band width can be derived from the SWA wave vector [23], but this gives only the limiting width for thick films. To obtain the dependence on thickness, one may calculate the optical spectra directly, and then extract the width numerically from these simulations [24].

The solid curves in Figs. 2 and 3 represent the results of these calculations. Parameters used here include the sphere diameter and number of sample layers, both determined from SEM measurements, and the dielectric constant of the silica spheres, determined using index matching experiments [inset to Fig. 3(a)]. In these experiments, the interstitial regions of a silica/air sample are filled with various fluids of known index; the peak optical density is smallest when the index of the fluid matches that of the spheres [25]. For chemically prepared silica nanospheres, the refractive index is generally less than the index of bulk SiO_2 [26]. Here, index matching with isopropanol ($n = 1.375$) gave the smallest optical density. This value is used as the index of the spheres in the calculations presented here. The agreement between theory and experiment is remarkable, given that the SWA assumes an ideal, defect-free lattice.

These results suggest that the broad bandwidths observed in these samples are a fundamental property of close-packed spherical arrays. This may be understood as follows. For crystals of high dielectric contrast, diffraction is very strong, and the amplitude of the radiation attenuates rapidly with propagation distance into the crystal. As a result, most of the incident radiation interacts only with a few lattice planes, near the surface. The measured bandwidth is determined largely by these interactions near the input facet, and not by the subsequent propagation through the medium. Thus, increasing the thickness of the crystal above a certain critical thickness has little effect on the bandwidth.

Zacharaisen has given an expression for the critical thickness, derived within the framework of dynamical diffraction theory [17]; however, this result is derived under the assumption of small dielectic contrast, and is therefore not valid for our systems. A more general result, valid for any ψ_0, can be found from the SWA, as follows.

The critical thickness N_c, expressed as the number of {111} layers, may be defined by $k^i_{\max} N_c d_{111} = 1$, where $k^i_{\max}$ is the imaginary part of the photon wave vector at the center of the stop band, and where d_{111} is the {111} lattice spacing. For close-packed spheres, N_c is given by

$$N_c = \frac{1}{\pi}\left[\sqrt{4 + \left(\frac{K\psi_0}{1 + \psi_0}\right)^2} - 2\right]^{-1/2},$$

where $K = (2/\beta^3)[\sin\beta - \beta\cos\beta]$, and where $\beta = 2\pi\sqrt{3/8}$. For the silica/air films, $N_c = 13$ layers, whereas for an air/polymer film made with PAMA ($n = 1.64$), $N_c = 6$ layers.

A consequence of this analysis is that, for a crystal of a given thickness, the bandwidth should be a sensitive function of the dielectric contrast. As mentioned previously, one can control the contrast by filling the interstitial pores of a silica colloidal crystal with dielectric fluids. In this way, a range of different values of ψ_0 can be obtained for a single sample [25]. As shown in the inset to Fig. 3(a), the peak width narrows as the dielectric contrast decreases from either direction. The solid line is obtained from the SWA calculations as described above.

The SWA prediction for the strength of the attenuation (Fig. 2, inset) is almost precisely a factor of 2 larger than the experimental result. This discrepancy, which is also manifested in air/polymer samples, could be related to the approximations inherent to the SWA. Alternatively, it might be associated with planar stacking faults along the {111} axis, a type of disorder known to be present in colloidal crystals [27]. In any event, it is clear from both theory and experiment that the evolution of this parameter does not change abruptly at $N = N_c$.

These results provide convincing evidence that broad stop-band widths are intrinsic to these structures. Since the bandwidth exhibits a dramatic change in behavior at the critical thickness while the peak attenuation does not, bandwidth is evidently a more reasonable characterization of the importance of film thickness in these systems. This understanding of the nature of the stop band offers a prescription for engineering materials with narrower bandwidths. One must increase the number of layers and also decrease the diffraction efficiency per layer. This can be achieved using a polymer to fill the interstitial regions, rather than dielectric fluids as in Fig. 3. Such materials provide a range of possibilities for engineered photonic systems.

This work was supported by the NSF (CHE-960720) and the Welch Foundation (C-1342).

*Email address: colvin@ruf.rice.edu

[1] E. Yablonovitch *et al.*, Opt. Quantum Electron. **24**, 273 (1992).
[2] P. Rundquist *et al.*, J. Chem. Phys. **91**, 4932 (1989).
[3] I. I. Tarhan and G. H. Watson, Phys. Rev. Lett. **76**, 315 (1996).
[4] W. L. Vos *et al.*, Phys. Rev. B **53**, 16 231 (1996).
[5] H. Miguez *et al.*, Appl. Phys. Lett. **71**, 1149 (1997).
[6] K. Osseo-Asare and F. J. Arriagada, Colloids Surf. **50**, 321 (1990).
[7] P. L. Flaugh, S. E. O'Donnell, and S. A. Asher, Appl. Spectrosc. **38**, 847 (1984).
[8] L. Carin *et al.*, IEEE J. Quantum Electron. **29**, 2141 (1993).
[9] E. Ozbay, J. Opt. Soc. Am. B **13**, 1945 (1996).
[10] P. Jiang *et al.*, Chem. Mater. (to be published).
[11] Y. A. Vlasov *et al.*, Appl. Phys. Lett. **71**, 1616 (1997).
[12] C. Herbert and M. Malcuit, Opt. Lett. **18**, 1783 (1993).
[13] G. Pan, R. Kesavamoorthy, and S. A. Asher, Phys. Rev. Lett. **78**, 3860 (1997).
[14] W. Stober, A. Fink, and E. Bohn, J. Colloid Interface Sci. **26**, 62 (1968).
[15] K. Yoshino *et al.*, Appl. Phys. Lett. **73**, 3506 (1998).
[16] P. Jiang *et al.* (to be published).
[17] W. H. Zachariasen, *Theory of X-Ray Diffraction in Crystals* (Dover Publications, New York, 1945).
[18] P. C. Becker, N. A. Olsson, and J. R. Simpson, *Erbium-Doped Fiber Amplifiers* (Academic Press, San Diego, 1999).
[19] J. D. Joannopoulos, R. D. Meade, and J. N. Winn, *Photonic Crystals: Molding the Flow of Light* (Princeton University Press, Princeton, New Jersey, 1995).
[20] S. Satpathy, Z. Zhang, and M. R. Salehpour, Phys. Rev. Lett. **64**, 1239 (1990).
[21] K. Shung and Y. Tsai, Phys. Rev. B **48**, 11 265 (1993).
[22] S. Datta *et al.*, Phys. Rev. B **48**, 14 936 (1993).
[23] I. Tarhan and G. Watson, Phys. Rev. B **54**, 7593 (1996).
[24] D. M. Mittleman *et al.*, J. Chem. Phys. **111**, 345 (1999).
[25] H. B. Lin, R. J. Tonucci, and A. J. Campillo, Appl. Phys. Lett. **68**, 2927 (1996).
[26] A. van Blaaderen and A. Vrij, Langmuir **8**, 2921 (1992).
[27] A. van Bladderen and P. Wiltzius, Science **270**, 1177 (1995).